Finite Element Analysis of Cracking Localization: The Smeared Crack Approach with a Mixed Formulation

Pruettha Nanakorn
Associate Professor, Civil Engineering Program
Sirindhorn International Institute of Technology
Thammasat University, Pathumthani 12121, Thailand

Preecha Soparat
Master's Degree Student, Civil Engineering Program
Sirindhorn International Institute of Technology
Thammasat University, Pathumthani 12121, Thailand

Abstract

In the analysis of cracking localization, consideration of stability and bifurcation of equilibrium states is necessary. Therefore, it is more suitable to have an energy expression written in terms of discrete irreversible variables, which will allow the variations of the energy with respect to the irreversible variables to be considered easily. This implies that, for this kind of analysis, the discrete crack approach should be appropriate. Nevertheless, the discrete crack approach may not be the best choice for problems with many cracks, which are unavoidable for the analysis of the cracking localization. In this aspect, the smeared crack approach may be more appropriate. To avoid this dilemma, a mixed finite element formulation based on the smeared crack finite element approach is proposed in this study. In the formulation, both displacement and crack strain fields are discretized. Consequently, the stability of crack patterns with respect to the discrete irreversible variables, which are the nodal local crack strain variables, can be easily investigated. This will allow the cracking localization to be discussed even when the smeared crack approach is used in the analysis.

1. Introduction

The failure of quasi-brittle materials such as concrete is known to start from the formation of cracks, and the propagation of the newly formed cracks or the existing defects. After that, localization of these cracks into one or a few major cracks will occur. This will subsequently lead to the final failure. The cracking localization prior to the failure plays a very important role in the fracture behavior of this kind of material. In order to capture the ultimate capacity of such materials in structures, consideration of the cracking localization cannot generally be neglected. However, consideration of the cracking localization needs very expensive computation because the localization problems involve checking stability and bifurcation of many different equilibrium paths. Massive eigenvalue analysis must be performed in every computational step. Because of this, many researchers avoid the consideration of the cracking localization either by allowing many cracks to open or grow without consideration of the localization [1, 2, 3, 4, 5] or by assuming the positions of the localized cracks [5, 6]. The first approach, though simple, is not realistic and can lead to very inaccurate results. When compared with having one or a few localized cracks, having many cracks without the localization allows different amounts of energy to dissipate from the domain. Thus, the obtained results will be different as well. Only in some cases where the stress gradients of the problems under consideration are very large and the stress criteria for crack initiation are used, can the localized solutions possibly be obtained from this approach [1, 2, 4]. The second approach, which assumes the locations of the localized cracks prior to the analysis, may also yield reasonable results in some cases. These include cases where the locations of the localized cracks can be easily predicted, such as bending

problems of concrete beams with long notches [6]. The others are cases where the required solutions, such as the ultimate loads, are not sensitive to the locations of the localized cracks [5]. However, this second approach is not appropriate for general cases since the locations of the localized cracks may not be easily predicted or the required solutions may be sensitive to the locations of the cracks.

In the analysis of the cracking localization, which involves irreversible processes, consideration of stability and bifurcation of equilibrium states with respect to irreversible parameters is one of the tasks to be done. Many researchers have considered the stability and bifurcation of the equilibrium states by investigating the definiteness of the stiffness matrices (Hessian Matrices) [7, 8, 9]. When the matrix is positive-definite, the equilibrium is stable. The same theory can be applied to the analysis of the cracking localization. However, cracking is an irreversible process. To consider stability and bifurcation of irreversible processes, the stationary condition of the energy of the system with respect to irreversible parameters has to be investigated [10, 11, 12]. For this reason, the expression of the energy in terms of the irreversible parameters is required. For crack problems, the irreversible parameters can be the discrete irreversible crack opening displacements in the discrete crack approach or the irreversible crack strains in the smeared crack approach. In the discrete crack approach, the crack opening displacements are usually discretized along crack paths and treated as the degrees of freedom in the analysis. The energy of the system can be expressed in terms of these degrees of freedom. Computing the first and second variations of the energy with respect to these discrete crack opening displacements can be done easily by employing ordinary calculus [12]. In the smeared crack approach, the energy is expressed in terms of irreversible crack strains, which are functions of position and are generally not discretized. To compute the first and second variations of the energy with respect to these crack strains, a complex mathematics involving the calculus of variations must be employed. This fact implies that the discrete crack approach in the finite element method may be more suitable for the cracking localization analysis than the smeared crack approach.

However, the discrete crack approach may not be the best choice for problems with many cracks. In the cracking localization analysis, there will be many cracks appearing in the domain. Having many cracks in the domain leads to many degrees of freedom. Furthermore, as the number of cracks increases, the mesh topology of the problem may have to be changed significantly to cope with the new crack patterns. In addition, the singularity problem of the system stiffness equation may also arise. These problems can be mostly avoided if the smeared crack approach is employed. In the smeared crack models, no increase in the number of the degrees of freedom or change in the mesh topology is required during the propagation of cracks. Although the smeared crack models may also face the singularity problem of the system in case of softening materials, the problem is less serious than that of the discrete crack models.

To avoid the drawbacks in both approaches, in this study, discrete irreversible variables are introduced in the smeared crack models. To this end, a mixed formulation of the finite element method that includes the discretization of the displacement and crack strain fields is proposed. The energy of the system is written in terms of the discretized displacements and crack strains. Consequently, the stability of crack patterns with respect to the discretized irreversible crack strains can be easily evaluated, and the cracking localization can be discussed.

In this paper, the derivation of the proposed mixed formulation is shown. After that, the validity of the proposed technique is checked by solving a benchmark uniaxial problem using one- and two-dimensional elements. The obtained results show promising capability of the method for the analysis of the cracking localization.

2. Mixed Finite Element Formulation for Analysis of Cracking Localization

The fundamental scheme of the smeared crack models [1, 13, 14] is the decomposition of the total strain increment $\Delta\varepsilon$ into the strain increments of an intact solid part $\Delta\varepsilon^{o}$ and a cracked part $\Delta\varepsilon^{cr}$, i.e.,

$$\Delta\varepsilon = \Delta\varepsilon^{o} + \Delta\varepsilon^{cr}. \qquad (1)$$

The strain increment vectors in the above equation are written in the global coordinate system. It will be helpful to consider the strain increments also in a local coordinate system that aligns with the crack. In two-dimensional cases, the local crack strain increment $\Delta\hat{\boldsymbol{\varepsilon}}^{cr}$ can be written as

$$\Delta\hat{\boldsymbol{\varepsilon}}^{cr} = \left[\Delta\hat{\varepsilon}_{nn}^{cr} \quad \Delta\hat{\gamma}_{nt}^{cr}\right]^T \tag{2}$$

where $\Delta\hat{\varepsilon}_{nn}^{cr}$ and $\Delta\hat{\gamma}_{nt}^{cr}$ are the normal and shear crack strain increments, respectively. The relationship between the global crack strain increment vector $\Delta\boldsymbol{\varepsilon}^{cr}$ and the local crack strain increment vector $\Delta\hat{\boldsymbol{\varepsilon}}^{cr}$ is expressed as

$$\Delta\boldsymbol{\varepsilon}^{cr} = \mathbf{T}\Delta\hat{\boldsymbol{\varepsilon}}^{cr} \tag{3}$$

where $\mathbf{T}$ is the transformation matrix between the global and local coordinate systems defined as

$$\mathbf{T} = \begin{bmatrix} \cos^2\theta & -\sin\theta\cos\theta \\ \sin^2\theta & \sin\theta\cos\theta \\ 2\sin\theta\cos\theta & \cos^2\theta - \sin^2\theta \end{bmatrix} \tag{4}$$

where θ is the angle between the vector normal to the crack surfaces and the global x-axis.

In the local coordinate system, we also have the local traction increment $\Delta\hat{\mathbf{t}}^{cr}$ across the crack defined as

$$\Delta\hat{\mathbf{t}}^{cr} = \left[\Delta\hat{t}_n^{cr} \quad \Delta\hat{s}_t^{cr}\right]^T \tag{5}$$

where $\Delta\hat{t}_n^{cr}$ and $\Delta\hat{s}_t^{cr}$ are normal and shear crack traction increments, respectively.

The constitutive models for the intact solid part and for the cracked part must be specified. For the intact solid part, we have

$$\Delta\boldsymbol{\sigma} = \mathbf{D}^o\Delta\boldsymbol{\varepsilon}^o \tag{6}$$

where $\mathbf{D}^o$ is the constitutive matrix for the intact solid. For the cracked part, we have the local traction-crack strain relationship, i.e.,

$$\Delta\hat{\mathbf{t}}^{cr} = \hat{\mathbf{D}}^{cr}\Delta\hat{\boldsymbol{\varepsilon}}^{cr} \tag{7}$$

where $\hat{\mathbf{D}}^{cr}$ is the crack constitutive matrix incorporating mixed-mode properties of the crack [1].

In order to discuss the cracking localization, we consider the total energy increment for a cracked domain V written as

$$\begin{aligned}\Delta\Pi &= \Delta\Pi^M + \Delta\Pi^D \\ &= \begin{bmatrix} \frac{1}{2}\int_V \Delta\boldsymbol{\varepsilon}^{oT}\Delta\boldsymbol{\sigma}dV - \int_S \Delta\mathbf{u}^T\Delta\mathbf{t}dS \\ -\int_V \Delta\mathbf{u}^T\Delta\mathbf{f}dV \end{bmatrix} \\ &\quad + \left[\frac{1}{2}\int_V \Delta\hat{\boldsymbol{\varepsilon}}^{crT}\Delta\hat{\mathbf{t}}^{cr}dV\right]\end{aligned} \tag{8}$$

where $\Delta\Pi^M$ and $\Delta\Pi^D$ represent the mechanical potential energy increment and the dissipated energy increment, respectively [10, 11, 12]. Here, $\Delta\mathbf{t}$ and $\Delta\mathbf{f}$ denote the surface traction increment vector and the body force increment vector, respectively.

Substituting Eqs. (6) and (7) into Eq. (8), we obtain

$$\begin{aligned}\Delta\Pi &= \begin{bmatrix} \frac{1}{2}\int_V \Delta\boldsymbol{\varepsilon}^{oT}\mathbf{D}^o\Delta\boldsymbol{\varepsilon}^o dV - \int_S \Delta\mathbf{u}^T\Delta\mathbf{t}dS \\ -\int_V \Delta\mathbf{u}^T\Delta\mathbf{f}dV \end{bmatrix} \\ &\quad + \left[\frac{1}{2}\int_V \Delta\hat{\boldsymbol{\varepsilon}}^{crT}\hat{\mathbf{D}}^{cr}\Delta\hat{\boldsymbol{\varepsilon}}^{cr}dV\right].\end{aligned} \tag{9}$$

In the expression for the total energy increment in Eq. (9), the irreversible variable that has to be considered in the stability analysis is the local crack strain increment $\Delta\hat{\boldsymbol{\varepsilon}}^{cr}$. The first variation of the total energy increment with respect to this local crack strain increment results in the equilibrium path. The second variation will give the information on the stability condition of the obtained equilibrium path. Since the total energy increment is a functional of the crack strain increment function, the calculus of variations is required. To avoid this difficulty, we employ the mixed formulation in the finite element method by discretizing both

displacement and local crack strain increments. For the i^{th} element in the finite element analysis, we have

$$\Delta\mathbf{u} = \mathbf{N}\Delta^i\mathbf{U} \tag{10a}$$

$$\Delta\hat{\boldsymbol{\varepsilon}}^{cr} = \mathbf{N}^{cr}\Delta^i\hat{\mathbf{E}}^{cr} \tag{10b}$$

where $\mathbf{N}$ and $\mathbf{N}^{cr}$ represent the shape function matrices for the displacement and local crack strain increments, respectively. In addition, $\Delta^i\mathbf{U}$ and $\Delta^i\hat{\mathbf{E}}^{cr}$ represent the nodal displacement and nodal local crack strain increment vectors, respectively.

Note that the local crack strain increments are not continuous across elements and the nodal local crack strain increments of the same node for different elements can be different. The continuity of the local crack strain increments between elements is not required and must not be enforced. One example is a problem with one cracked element surrounded by uncracked elements. In the cracked element including its boundary, non-zero crack strain increments (see Fig. 1) can be expected. However, in the surrounding uncracked elements, the crack strain increments are expected to be zero because there is no crack in those elements. On the contrary, the total displacement increments must be continuous across the elements.

By substituting Eq. (1) into Eq. (9), the total energy increment for the i^{th} element is rewritten as

$$\begin{aligned}\Delta\Pi = &\frac{1}{2}\int_V\left(\Delta\boldsymbol{\varepsilon}-\Delta\boldsymbol{\varepsilon}^{cr}\right)^T\mathbf{D}^o\left(\Delta\boldsymbol{\varepsilon}-\Delta\boldsymbol{\varepsilon}^{cr}\right)dV\\ &+\frac{1}{2}\int_V\Delta\hat{\boldsymbol{\varepsilon}}^{cr\,T}\hat{\mathbf{D}}^{cr}\Delta\hat{\boldsymbol{\varepsilon}}^{cr}dV\\ &-\int_V\Delta\mathbf{u}^T\Delta\mathbf{f}dV-\int_S\Delta\mathbf{u}^T\Delta\mathbf{t}dS.\end{aligned} \tag{11}$$

From Eq. (10a), we write the total strain increment in terms of the nodal displacement increment, i.e.,

$$\Delta\boldsymbol{\varepsilon} = \mathbf{B}\Delta^i\mathbf{U}\,. \tag{12}$$

Substituting Eq. (10b) into Eq. (3) yields

$$\Delta\boldsymbol{\varepsilon}^{cr} = \mathbf{T}\mathbf{N}^{cr}\Delta^i\hat{\mathbf{E}}^{cr}. \tag{13}$$

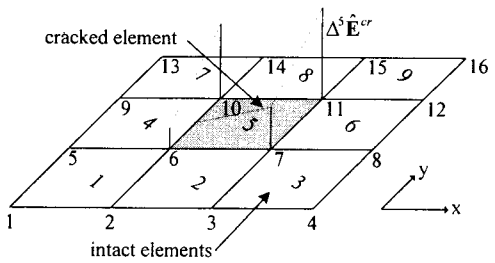

Fig. 1 A problem with one cracked element surrounded by uncracked elements

Substituting Eqs. (12) and (13) into Eq. (11), we get

$$\begin{aligned}\Delta\Pi = &\frac{1}{2}\int_V\Delta^i\mathbf{U}^T\mathbf{B}^T\mathbf{D}^o\mathbf{B}\Delta^i\mathbf{U}dV\\ &-\frac{1}{2}\int_V\Delta^i\mathbf{U}^T\mathbf{B}^T\mathbf{D}^o\mathbf{T}\mathbf{N}^{cr}\Delta^i\hat{\mathbf{E}}^{cr}dV\\ &-\frac{1}{2}\int_V\Delta^i\hat{\mathbf{E}}^{cr\,T}\mathbf{N}^{cr\,T}\mathbf{T}^T\mathbf{D}^o\mathbf{B}\Delta^i\mathbf{U}dV\\ &+\frac{1}{2}\int_V\Delta^i\hat{\mathbf{E}}^{cr\,T}\mathbf{N}^{cr\,T}\mathbf{T}^T\mathbf{D}^o\mathbf{T}\mathbf{N}^{cr}\Delta^i\hat{\mathbf{E}}^{cr}dV\\ &+\frac{1}{2}\int_V\Delta^i\hat{\mathbf{E}}^{cr\,T}\mathbf{N}^{cr\,T}\hat{\mathbf{D}}^{cr}\mathbf{N}^{cr}\Delta^i\hat{\mathbf{E}}^{cr}dV\\ &-\int_V\Delta^i\mathbf{U}^T\mathbf{N}^T\Delta\mathbf{f}dV-\int_S\Delta^i\mathbf{U}^T\mathbf{N}^T\Delta\mathbf{t}dS.\end{aligned} \tag{14}$$

Applying the stationary condition to Eq. (14) and assuming that both $\mathbf{D}^o$ and $\mathbf{D}^{cr}$ are symmetric, we get

$$\begin{aligned}\delta(\Delta\Pi) = &\delta\left(\Delta^i\mathbf{U}^T\right)\int_V\mathbf{B}^T\mathbf{D}^o\mathbf{B}dV\Delta\mathbf{U}\\ &-\delta\left(\Delta^i\mathbf{U}^T\right)\int_V\mathbf{B}^T\mathbf{D}^o\mathbf{T}\mathbf{N}^{cr}dV\Delta^i\hat{\mathbf{E}}^{cr}\\ &-\delta\left(\Delta^i\hat{\mathbf{E}}^{cr\,T}\right)\int_V\mathbf{N}^{cr\,T}\mathbf{T}^T\mathbf{D}^o\mathbf{B}dV\Delta^i\mathbf{U}\\ &+\delta\left(\Delta^i\hat{\mathbf{E}}^{cr\,T}\right)\int_V\mathbf{N}^{cr\,T}\mathbf{T}^T\mathbf{D}^o\mathbf{T}\mathbf{N}^{cr}dV\Delta^i\hat{\mathbf{E}}^{cr}\\ &+\delta\left(\Delta^i\hat{\mathbf{E}}^{cr\,T}\right)\int_V\mathbf{N}^{cr\,T}\hat{\mathbf{D}}^{cr}\mathbf{N}^{cr}dV\Delta^i\hat{\mathbf{E}}^{cr}\\ &-\delta\left(\Delta^i\mathbf{U}^T\right)\int_V\mathbf{N}^T\Delta\mathbf{f}dV\\ &-\delta\left(\Delta^i\mathbf{U}^T\right)\int_S\mathbf{N}^T\Delta\mathbf{t}dS\\ &=0.\end{aligned} \tag{15}$$

Since $\delta(\Delta^t\mathbf{U}^T)$ and $\delta(\Delta^t\hat{\mathbf{E}}^{cr\,T})$ are arbitrary, we obtain the element stiffness equation for the i^{th} element, i.e.,

$$\begin{bmatrix}\mathbf{k}_{11} & \mathbf{k}_{12}\\ \mathbf{k}_{21} & \mathbf{k}_{22}\end{bmatrix}\begin{Bmatrix}\Delta^t\mathbf{U}\\ \Delta^t\hat{\mathbf{E}}^{cr}\end{Bmatrix}=\begin{Bmatrix}\Delta\mathbf{r}\\ 0\end{Bmatrix} \tag{16}$$

where

$$\begin{aligned}\mathbf{k}_{11} &= \int_V \mathbf{B}^T\mathbf{D}^o\mathbf{B}dV\\ \mathbf{k}_{12} &= -\int_V \mathbf{B}^T\mathbf{D}^o\mathbf{T}\mathbf{N}^{cr}dV\\ \mathbf{k}_{21} &= -\int_V \mathbf{N}^{cr\,T}\mathbf{T}^T\mathbf{D}^o\mathbf{B}dV\\ \mathbf{k}_{22} &= \int_V \mathbf{N}^{cr\,T}\left(\hat{\mathbf{D}}^{cr}+\mathbf{T}^T\mathbf{D}^o\mathbf{T}\right)\mathbf{N}^{cr}dV\\ \Delta\mathbf{r} &= \int_V \mathbf{N}^T\Delta\mathbf{f}dV+\int_S \mathbf{N}^T\Delta\mathbf{t}dS.\end{aligned} \tag{17}$$

After assembling all element stiffness equations and applying prescribed displacements and forces, we arrange the system stiffness equation in the following form, i.e.,

$$\begin{bmatrix}\mathbf{K}_{11} & \mathbf{K}_{12}\\ \mathbf{K}_{21} & \mathbf{K}_{22}\end{bmatrix}\begin{Bmatrix}\Delta\mathbf{U}\\ \Delta\hat{\mathbf{E}}^{cr}\end{Bmatrix}=\begin{Bmatrix}\Delta\mathbf{R}_1\\ \Delta\mathbf{R}_2\end{Bmatrix} \tag{18}$$

where $\Delta\mathbf{U}$ and $\Delta\hat{\mathbf{E}}^{cr}$ represent, respectively, the nodal displacement increment and nodal local crack strain increment vectors for the system stiffness equation.

The static condensation is then used to remove the nodal displacement increment from the obtained system stiffness equation. Consequently, the equation can be written in the following form, i.e.,

$$\mathbf{K}^{cr}\Delta\hat{\mathbf{E}}^{cr}=\Delta\mathbf{R}^{cr} \tag{19}$$

where $\mathbf{K}^{cr}$ and $\Delta\mathbf{R}^{cr}$ are defined as

$$\begin{aligned}\mathbf{K}^{cr} &= \mathbf{K}_{22}-\mathbf{K}_{21}\mathbf{K}_{11}^{-1}\mathbf{K}_{12}\\ \Delta\mathbf{R}^{cr} &= \Delta\mathbf{R}_2-\mathbf{K}_{21}\mathbf{K}_{11}^{-1}\Delta\mathbf{R}_1.\end{aligned} \tag{20}$$

To investigate the stability of crack patterns, we compute the eigenvalues of $\mathbf{K}^{cr}$. If all of the eigenvalues are positive, it means that the solution is stable with respect to the current crack pattern. Otherwise, the solution is unstable and bifurcation occurs [10, 11, 15]. This will finally result in the localization of the cracks. Note that the proposed scheme is not used to obtain the displacement solution. The scheme is used only for stability consideration. The displacement solution will be obtained from the original smeared crack model where the only basic unknowns are the nodal displacements.

3. Results

In order to illustrate the advantage of the proposed method in the analysis of the cracking localization, a simple one-dimensional uniaxial problem shown in Fig. 2 is considered. The bar has one fixed support at one end. At the other end, the controlled displacement $\bar{u}$ is applied (see Fig. 2a). The length of the bar is $2L$ and the area is A. The material is assumed to be elastic with Young's modulus equal to E (see Fig. 2c). The bar is discretized into two elements, each of which has the length of L (see Fig. 2a). Each element can accommodate one crack. The characteristic length of each crack is equal to the length of the element. The conventional linear shape function is used for the displacement and local crack strain interpolations.

Assume no crack at the beginning. After that, the controlled displacement $\bar{u}$ is increased until the stress in the bar reaches the tensile strength f_t. By the strength criterion, both elements are cracked (see Fig. 2b), and they are changed from the elastic elements into the smeared crack elements. Thereafter, the cracks follow the constitutive law for cracks (see Fig. 2d). For opening cracks, a linear relationship between the transmitted tensile stress and the crack opening displacement (COD) with the slope $\dfrac{\Delta\sigma}{\Delta\mathrm{COD}}$ equal to H is assumed. Since, for ordinary cracks, softening behavior is always observed ($H<0$), this relationship is called the tension-softening relationship. It can be seen from the tension-softening relationship ($H<0$) that when a crack opens wider, the tensile stress transmitted across the crack decreases. This tension-softening relationship, which is used for all opening cracks, is also called the loading path.

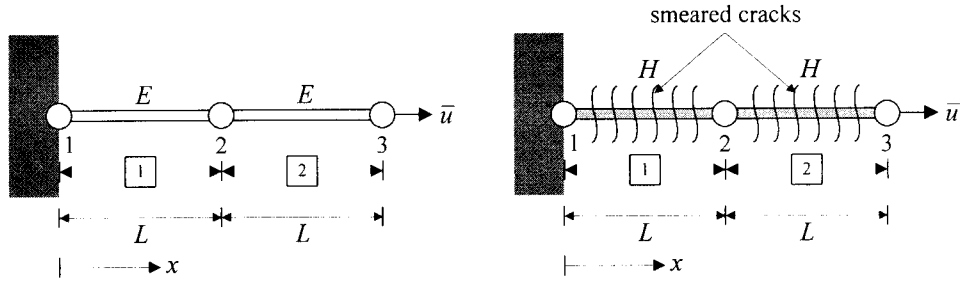

cross-sectional area = A

a) Before cracking

cross-sectional area = A

b) After cracking

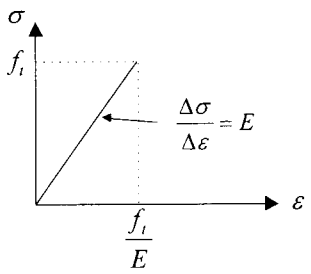

c) Constitutive law for intact solid

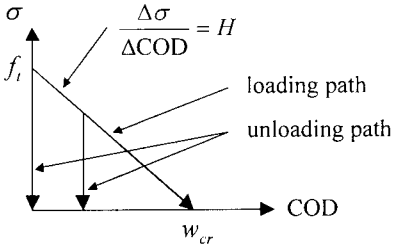

d) Constitutive law for cracks (tension-softenning curve)

Fig. 2 Uniaxial problem using one-dimensional bar elements

Generally, during loading, there may be some cracks that stop opening. These cracks are the unloading cracks. When a crack stops opening, its COD stops increasing. In this study, cracking is assumed to be an irreversible process, which means that CODs will not decrease. Therefore, each of these cracks will follow a vertical unloading path with a constant COD equal to the current COD that the crack has just before the unloading occurs (see Fig. 2d). For cracks with different CODs when the unloading occurs, different vertical unloading paths will be used.

Consider an incremental step after the initiation of the cracks. Note that both elements are now the smeared crack elements. Assembling all element stiffness equations given by Eq. (16), we write the system stiffness equation as

$$A\begin{bmatrix} \frac{E}{L} & -\frac{E}{L} & 0 & \frac{E}{2} & \frac{E}{2} & 0 & 0 \\ -\frac{E}{L} & \frac{2E}{L} & -\frac{E}{L} & -\frac{E}{2} & -\frac{E}{2} & \frac{E}{2} & \frac{E}{2} \\ 0 & -\frac{E}{L} & \frac{E}{L} & 0 & 0 & -\frac{E}{2} & -\frac{E}{2} \\ \frac{E}{2} & -\frac{E}{2} & 0 & \frac{(E+\tilde{H})L}{3} & \frac{(E+\tilde{H})L}{6} & 0 & 0 \\ \frac{E}{2} & -\frac{E}{2} & 0 & \frac{(E+\tilde{H})L}{6} & \frac{(E+\tilde{H})L}{3} & 0 & 0 \\ 0 & \frac{E}{2} & -\frac{E}{2} & 0 & 0 & \frac{(E+\tilde{H})L}{3} & \frac{(E+\tilde{H})L}{6} \\ 0 & \frac{E}{2} & -\frac{E}{2} & 0 & 0 & \frac{(E+\tilde{H})L}{6} & \frac{(E+\tilde{H})L}{3} \end{bmatrix} \begin{Bmatrix} \Delta U_1 \\ \Delta U_2 \\ \Delta U_3 \\ \Delta^1\hat{E}_1^{cr} \\ \Delta^1\hat{E}_2^{cr} \\ \Delta^2\hat{E}_2^{cr} \\ \Delta^2\hat{E}_3^{cr} \end{Bmatrix} = \begin{Bmatrix} \Delta R_1 \\ \Delta R_2 \\ \Delta R_3 \\ 0 \\ 0 \\ 0 \\ 0 \end{Bmatrix} \tag{21}$$

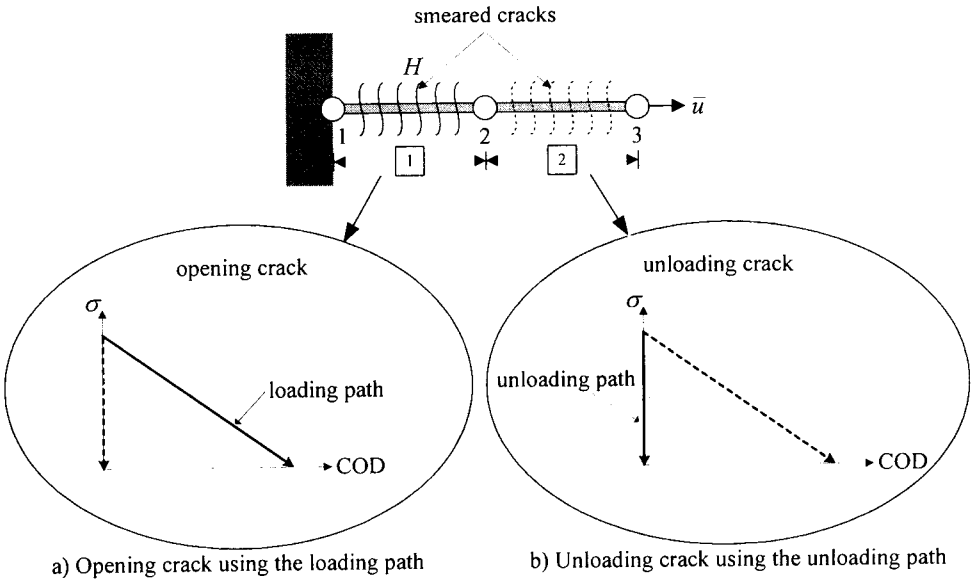

Fig. 3 Solution with one unloading crack

where $\tilde{H} = \dfrac{\Delta\sigma}{\Delta\varepsilon^{cr}} = HL^{*} = HL$. Here, L^{*} represents the characteristic length of the crack and is equal to L. In addition, ΔU_i and ΔR_i represent the nodal displacement increment and the nodal force increment of the node i, respectively. Moreover, $\Delta^{l}\hat{E}_j^{cr}$ represents the nodal local crack strain increment of the node j and, at the same time, of the element i.

Since ΔU_1, ΔU_3 and ΔR_2 are prescribed, the equation can be reduced into

$$A\begin{bmatrix} \frac{2E}{L} & -\frac{E}{2} & -\frac{E}{2} & \frac{E}{2} & \frac{E}{2} \\ -\frac{E}{2} & \frac{(E+\tilde{H})L}{3} & \frac{(E+\tilde{H})L}{6} & 0 & 0 \\ -\frac{E}{2} & \frac{(E+\tilde{H})L}{6} & \frac{(E+\tilde{H})L}{3} & 0 & 0 \\ \frac{E}{2} & 0 & 0 & \frac{(E+\tilde{H})L}{3} & \frac{(E+\tilde{H})L}{6} \\ \frac{E}{2} & 0 & 0 & \frac{(E+\tilde{H})L}{6} & \frac{(E+\tilde{H})L}{3} \end{bmatrix} \begin{Bmatrix} \Delta U_2 \\ \Delta^{1}\hat{E}_1^{cr} \\ \Delta^{1}\hat{E}_2^{cr} \\ \Delta^{2}\hat{E}_2^{cr} \\ \Delta^{2}\hat{E}_3^{cr} \end{Bmatrix}$$

$$= AE\begin{Bmatrix} \frac{\Delta\bar{u}}{L} \\ 0 \\ 0 \\ \frac{\Delta\bar{u}}{2} \\ \frac{\Delta\bar{u}}{2} \end{Bmatrix}. \qquad (22)$$

Using the static condensation to remove ΔU_2, we get

$$\frac{AL}{24}\begin{bmatrix} (5E+8\tilde{H}) & (E+4\tilde{H}) & 3E & 3E \\ (E+4\tilde{H}) & (5E+8\tilde{H}) & 3E & 3E \\ 3E & 3E & (5E+8\tilde{H}) & (E+4\tilde{H}) \\ 3E & 3E & (E+4\tilde{H}) & (5E+8\tilde{H}) \end{bmatrix} \begin{Bmatrix} \Delta^{1}\hat{E}_1^{cr} \\ \Delta^{1}\hat{E}_2^{cr} \\ \Delta^{2}\hat{E}_2^{cr} \\ \Delta^{2}\hat{E}_3^{cr} \end{Bmatrix}$$

$$= \frac{A}{4}\begin{Bmatrix} E\Delta\bar{u} \\ E\Delta\bar{u} \\ E\Delta\bar{u} \\ E\Delta\bar{u} \end{Bmatrix}. \qquad (23)$$

The eigenvalues of the obtained stiffness matrix are $\dfrac{A\tilde{H}L}{2}$, $\dfrac{A(E+\tilde{H})L}{6}$, $\dfrac{A(E+\tilde{H})L}{6}$ and $\dfrac{A(E+\tilde{H})L}{2}$. All eigenvalues will be positive only when $\tilde{H} > 0$. This means that the crack pattern having two cracks opening at the same time is unstable unless hardening behavior occurs at the cracks ($\tilde{H} > 0$). In reality, cracks will exhibit softening behavior. As a result, the two cracks cannot continue to open at the same time.

If we assume that the crack in the element 2 undergoes the elastic unloading, this crack will follow the vertical unloading path

shown in Fig. 3b. The crack in the element 1, which still continues to open, will follow the loading path shown in Fig. 3a. Note, in Fig. 3b, that the unloading path for the crack in the element 2 has the COD equal to zero. This is because, at the current state, the cracks in both elements are just initiated and the CODs are still exactly equal to zero. Remember that an incremental step after the initiation of the cracks is being considered and the stable solution path for this incremental step is being searched. With the crack in the element 2 unloading, the system stiffness equation will contain only one crack element, i.e.,

$$A\begin{bmatrix} \frac{E}{L} & -\frac{E}{L} & 0 & \frac{E}{2} & \frac{E}{2} \\ -\frac{E}{L} & \frac{2E}{L} & -\frac{E}{L} & -\frac{E}{2} & -\frac{E}{2} \\ 0 & -\frac{E}{L} & \frac{E}{L} & 0 & 0 \\ \frac{E}{2} & -\frac{E}{2} & 0 & \frac{(E+\tilde{H})L}{3} & \frac{(E+\tilde{H})L}{6} \\ \frac{E}{2} & -\frac{E}{2} & 0 & \frac{(E+\tilde{H})L}{6} & \frac{(E+\tilde{H})L}{3} \end{bmatrix} \begin{Bmatrix} \Delta U_1 \\ \Delta U_2 \\ \Delta U_3 \\ \Delta^1 \hat{E}_1^{cr} \\ \Delta^1 \hat{E}_2^{cr} \end{Bmatrix} = \begin{Bmatrix} \Delta R_1 \\ \Delta R_2 \\ \Delta R_3 \\ 0 \\ 0 \end{Bmatrix}. \tag{24}$$

Employing the same process of applying the prescribed boundary conditions and using the static condensation, we obtain

$$\frac{AL}{24}\begin{bmatrix} (5E+8\tilde{H})(E+4\tilde{H}) \\ (E+4\tilde{H})(5E+8\tilde{H}) \end{bmatrix} \begin{Bmatrix} \Delta^1 \hat{E}_1^{cr} \\ \Delta^1 \hat{E}_2^{cr} \end{Bmatrix} = \frac{A}{4}\begin{Bmatrix} E\Delta\bar{u} \\ E\Delta\bar{u} \end{Bmatrix}. \tag{25}$$

The eigenvalues of the stiffness matrix are $\frac{A(E+\tilde{H})L}{6}$ and $\frac{A(E+2\tilde{H})L}{4}$. Both will be positive at the same time only when $\tilde{H} > -\frac{E}{2}$. Assuming that the crack in the element 1 undergoes the elastic unloading will yield the same result.

In summary, immediately after the two elements are cracked due to the strength criterion employed, the equilibrium path with two opening cracks is unstable and bifurcation occurs unless the two cracks exhibit hardening behavior, i.e., when $H > 0$. In reality, cracks will exhibit softening behavior. Therefore, the two cracks cannot continue to open at the same time. If one of the cracks undergoes the elastic unloading, the stable equilibrium path can be observed as long as $H > -\frac{E}{2L}$. In the case of $H < -\frac{E}{2L}$, even the equilibrium path with one opening crack is not stable. Fig. 4 schematically shows the responses, obtained from the original smeared crack finite element model, for different cases of consideration. For this uniaxial problem, the responses obtained from the finite element model are exact since the linear shape function used in each element can exactly represent the exact displacement solutions, which are piecewise-linear functions of the axial coordinate. Note that the exact solutions mean

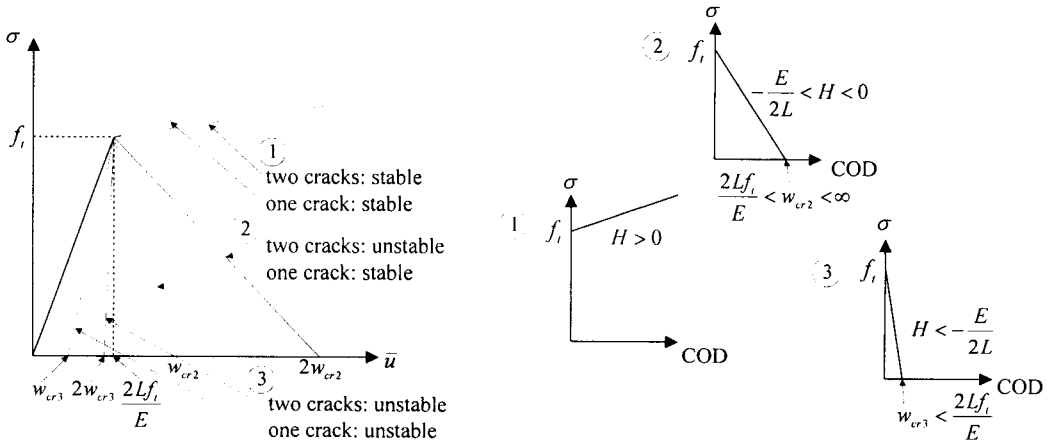

Fig. 4 Responses of the uniaxial problem using one-dimensional bar elements

the solutions that are obtained exactly from the equilibrium although they may not be stable. From Fig. 4, it can be seen that, when there is one opening crack and $H < -\frac{E}{2L}$, the obtained responses are the responses with snapback behavior. Under the displacement control, the snapback responses are always unstable.

Next, consider a uniaxial problem shown in Fig. 5. Same as the previous problem, the bar has a fixed support at one end and the displacement is controlled at the other end. However, this time, the two-dimensional elements will be used. The dimensions of the bar are as shown in the figure. The material is assumed to be elastic with Young's Modulus and Poisson's ratio equal to 25,000 and 0, respectively. The bar is discretized into two four-noded quadrilateral elements as also shown in the same figure. Each element can accommodate one crack. Since the alignment of each crack will be vertical and the elements are perfect rectangles, the characteristic length of each crack is equal to the horizontal dimension of the element. The conventional bilinear shape function is used for the displacement and local crack strain interpolations.

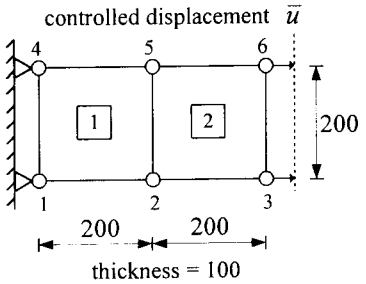

a) Before cracking

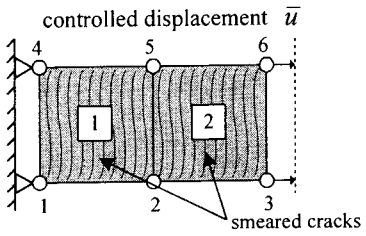

b) After cracking

Fig. 5 Uniaxial problem using two-dimensional elements

The controlled displacement $\bar{u}$ is increased until the tensile stress in the bar reaches the tensile strength f_t, which initiates the cracks in both elements. After that, opening cracks are assumed to follow the constitutive law for cracks defined by Eq. (7). For this problem, the crack constitutive matrix $\hat{\mathbf{D}}^{cr}$ is expressed as

$$\hat{\mathbf{D}}^{cr} = \begin{bmatrix} \tilde{H} & 0 \\ 0 & \tilde{G} \end{bmatrix} \tag{26}$$

where $\tilde{H}$ and $\tilde{G}$ represent the mode I and mode II crack modulus, respectively.

Since the problem is purely uniaxial and there will be only mode I cracking, the parameter $\tilde{G}$ is irrelevant and a small value (0.00001) is used just to prevent spurious mode II instability. For mode I cracking, various linear tension-softening relationships shown in Fig. 6 are investigated. First, the tension-softening curve *A*, which has the critical crack opening displacement equal to 0.05, is used. Note that the critical crack opening displacement is the crack opening displacement at which the stress-free crack occurs. For this tension-softening curve, $\tilde{H} = \frac{\Delta\sigma_{nn}}{\Delta\hat{\varepsilon}_{nn}^{cr}}$ is equal to $HL^* = \left(-\frac{2}{0.05}\right)200$.

Again, consider an incremental step after the initiation of the cracks. After assembling all element stiffness equations and applying all prescribed boundary conditions, the static condensation is used to remove all nodal displacement degrees of freedom and the stiffness $\mathbf{K}^{cr}$ in Eq. (19) is obtained. Since two

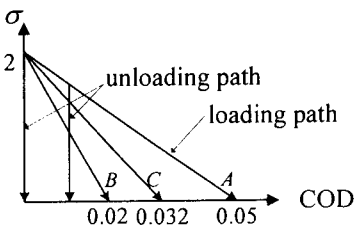

Fig. 6 Tension-softening curves for the problem using two-dimensional elements

opening cracks are being assumed, there will be totally 16 local crack strain increment degrees of freedom, eight from each of the two elements. Therefore, $\mathbf{K}^{cr}$ is a 16×16 matrix. The eigenvalue analysis is performed on $\mathbf{K}^{cr}$ and the eigenvalues are obtained as

$$\begin{bmatrix} 5.6667\times10^{9} \\ 5.6667\times10^{9} \\ 5.6667\times10^{9} \\ 1.8889\times10^{9} \\ 1.8889\times10^{9} \\ 1.3889\times10^{9} \\ 1.3889\times10^{9} \\ 10.000 \\ 10.000 \\ 1.7000\times10^{10} \\ -8.0000\times10^{9} \\ 4.0569\times10^{9} \\ 4.1667\times10^{9} \\ 4.5257\times10^{9} \\ 3.1326\times10^{9} \\ -1.6368\times10^{9} \end{bmatrix}$$

Since not all eigenvalues are positive, the current crack pattern is not stable. Therefore, one of the cracks must undergo the elastic unloading. The element that undergoes the elastic unloading is incrementally considered as an elastic element without crack. In this problem, there are again two alternatives since either of the two elements can be selected as the unloading element. Both alternatives are investigated and the eigenvalues of the modified stiffness matrices $\mathbf{K}^{cr}$ for both cases are obtained as

Opening crack in the first element	Opening crack in the second element
$\begin{bmatrix} 4.5000\times10^{9} \\ 1.8889\times10^{9} \\ 5.6667\times10^{9} \\ 4.5997\times10^{9} \\ 1.7614\times10^{9} \\ 1.3889\times10^{9} \\ 3.9216\times10^{9} \\ 10.000 \end{bmatrix}$	$\begin{bmatrix} 1.8889\times10^{9} \\ 4.5000\times10^{9} \\ 5.6667\times10^{9} \\ 1.7614\times10^{9} \\ 1.3889\times10^{9} \\ 3.2680\times10^{9} \\ 4.5997\times10^{9} \\ 10.000 \end{bmatrix}$

It can be seen that the solutions with only one opening crack are stable because all the eigenvalues are positive. It is interesting to check whether the solutions with one opening crack will be always stable even for different tension-softening curves. From the previous problem, it is found that steep tension-softening curves can lead to unstable one-opening-crack solutions. To investigate this matter, the tension-softening curves B and C in Fig. 6 are tried. In these B and C cases, $\tilde{H}$ is equal to $\left(-\frac{2}{0.02}\right)200$ and $\left(-\frac{2}{0.032}\right)200$, respectively. From the eigenvalue analyses, the eigenvalues of the stiffness matrices $\mathbf{K}^{cr}$ for the case B are obtained as

Opening crack in the first element	Opening crack in the second element
$\begin{bmatrix} 1.6667\times10^{9} \\ 5.5556\times10^{8} \\ -7.5000\times10^{9} \\ 1.3889\times10^{9} \\ 10.000 \\ 3.8603\times10^{9} \\ 3.9216\times10^{9} \\ -1.4991\times10^{9} \end{bmatrix}$	$\begin{bmatrix} 5.5556\times10^{8} \\ 1.6667\times10^{9} \\ -7.5000\times10^{9} \\ 1.3889\times10^{9} \\ 10.000 \\ 3.2680\times10^{9} \\ 3.8603\times10^{9} \\ -1.4991\times10^{9} \end{bmatrix}$

In addition, the eigenvalues for the case C are obtained as

Opening crack in the first element	Opening crack in the second element
$\begin{bmatrix} 1.3889\times10^{9} \\ 1.3889\times10^{9} \\ -2.1458\times10^{-6} \\ 10.000 \\ 4.1667\times10^{9} \\ 4.1667\times10^{9} \\ 6.9444\times10^{8} \\ 3.9216\times10^{9} \end{bmatrix}$	$\begin{bmatrix} 1.3889\times10^{9} \\ 1.3889\times10^{9} \\ -1.9667\times10^{-6} \\ 4.1667\times10^{9} \\ 10.000 \\ 4.1667\times10^{9} \\ 6.9444\times10^{8} \\ 3.2680\times10^{9} \end{bmatrix}$

From the result, it can be seen that the tension-softening curve B yields unstable solutions even when there is only one opening crack. As for the tension-softening curve C, one of the obtained eigenvalues in each of the two solutions is very small compared to the rest of

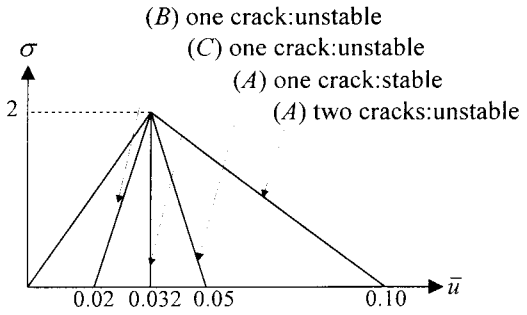

Fig. 7 Responses of the uniaxial problem for various tension-softening curves

the eigenvalues and must actually be considered as a zero. Therefore, the tension-softening curve C actually defines a boundary between stable and unstable one-opening-crack solutions. For those cases with tension-softening curves steeper than the curve C (e.g. the curve B), the solutions with one opening crack are not stable and they are in fact the snap-back responses. For those cases with tension-softening curves flatter than the curve C (e.g. the curve A), the solutions with one opening crack are stable. Note that the same tensile strength is assumed for all cases.

Fig. 7 shows the responses, obtained from the smeared crack finite element model, for all cases A, B and C. For the case A, the response without the localization is also plotted. Similar to the previous example, these results are also exact because the shape function used is capable of representing the exact solutions of this problem. From the results, it is clear that the localization judgment is necessary if the accurate solution is to be obtained.

4. Conclusion

The smeared crack approach can be used in the analysis of the cracking localization by employing the mixed formulation in the finite element method. In the formulation, the displacements and crack strains are both discretized. The discretization of the crack strains, which are the irreversible variables, allows the consideration of stability and bifurcation of equilibrium states with respect to the irreversible variables to be done easily. Therefore, the cracking localization can be subsequently discussed. The technique is tried with an axial bar problem employing both one-dimensional two-noded and two-dimensional four-noded elements. The obtained results show promising capability of the method for the analysis of the cracking localization.

5. Acknowledgments

The authors are grateful to the Thailand Research Fund (TRF) for providing the financial support to this study.

6. References

[1] Rots, J. G. and de Borst, R. Analysis of Mixed-Mode Fracture in Concrete, Journal of Engineering Mechanics, Vol.113, No.11, pp.1739-1758, 1987.

[2] Rots, J. G., Stress Rotation and Stress Locking in Smeared Analysis of Separation, Fracture Toughness and Fracture Energy: Test Methods for Concrete and Rock, H. Takahashi, Folker H. Wittmann and H. Mihashi (Eds.), Balkema, Rotterdam, pp.367-382, 1989.

[3] Dvorkin, E. N. and Assanelli, A. P., 2D Finite Elements with Displacement Interpolated Embedded Localization Lines: The Analysis of Fracture in Frictional Materials, Computer Methods in Applied Mechanics and Engineering, Vol.90, pp.829-844, 1991.

[4] Jirasek, M. and Zimmermann, T., Rotating Crack Model with Transition to Scalar Damage, Journal of Engineering Mechanics, Vol.124, No.3, pp.277-284, 1998.

[5] Shirai, N., JCI round robin analysis of size effect in concrete structures, Size Effect in Concrete Structures, H. Mihashi, H. Okamura and Z. P. Bazant (Eds.), E&FN Spon, London, pp.295-322, 1994.

[6] Carpinteri, A., Softening and Snap-Back Instability in Cohesive Solids, International Journal for Numerical Methods in Engineering, Vol.28, pp.1521-1537 , 1989.

[7] Riks, E., An Incremental Approach to the Solution of Snapping and Buckling Problems, Int. J. Solids Structures, Vol.15, pp.529-551, 1979.

[8] de Borst, R., Computation of Post-Bifurcation and Post-Failure Behavior of Strain-Softening Solids, Computers and Structures, Vol.25, No.2, pp.211-224, 1987.

[9] Valente, S., Bifurcation Phenomena in Cohesive Crack Propagation, Computers

and Structures, Vol.44, No.1/2, pp.55-62 , 1992.

[10] Nguyen, Q. S., Bifurcation and Post-Bifurcation Analysis in Plasticity and Brittle Fracture, J. Mech. Phys. Solids, Vol.35, No.3, pp.303-324, 1987.

[11] Horii, H. and Okui, Y., Thermomechanics and Micromechanics-Based Continuum Theory for Localization Phenomena, Fracture of Brittle, Disordered Materials: Concrete, Rock, and Ceramics, G. Baker and B. L. Karihaloo (Eds.), E&FN Spon, London. pp.391-405, 1995.

[12] Brocca, M., Analysis of Cracking Localization and Crack Growth Based on Thermomechanical Theory of Localization. Master of Engineering Thesis, The University of Tokyo, Tokyo, 1997.

[13] Bazant, Z. P. and Oh, B. H., Crack Band Theory for Fracture of Concrete, Materiaux et Constructions, Vol.16, No.93, pp.155-177, 1983.

[14] Shah, S. P., Swartz, S. E. and Ouyang, C., Fracture Mechanics of Concrete: Applications of Fracture Mechanics to Concrete, Rock, and Other Quasi-Brittle Materials, John Wiley & Sons, New York, 1995.

[15] Bazant, Z. P. and Cedolin, L., Stability of Structures: Elastic, Inelastic, Fracture, and Damage Theories, Oxford University Press, New York, 1991.